Stimulated Rayleigh-Bragg scattering in two-photon absorbing media

Guang S. He, Changgui Lu, Qingdong Zheng, and Paras N. Prasad
The Institute for Lasers, Photonics and Biophotonics, State University of New York at Buffalo, Buffalo, New York 14260, USA

Petros Zerom and Robert W. Boyd
The Institute of Optics, University of Rochester, Rochester, New York 14627, USA

Marek Samoc
Laser Physics Centre, The Australian National University, Canberra, Australian Capital Territory 0200, Australia
(Received 14 August 2004; revised manuscript received 7 March 2005; published 17 June 2005)

The origin and mechanism of backward stimulated Rayleigh scattering in two-photon absorbing media are studied theoretically and experimentally. This type of stimulated scattering has the unusual features of no frequency shift and low pump threshold requirement compared to all other known stimulated scattering effects. This frequency-unshifted stimulated Rayleigh scattering effect can be well explained by a two-photon-excitation-enhanced Bragg grating reflection model. The reflection of the forward pump beam from this stationary Bragg grating may substantially enhance the backward Rayleigh scattering beam, providing a positive feedback mechanism without causing any frequency shift. A two-counterpropagating-beam-formed grating experiment in a two-photon absorbing dye solution is conducted. The measured dynamic behavior of Bragg grating formation and reflectivity properties are basically consistent with the predictions from the proposed model.

DOI: 10.1103/PhysRevA.71.063810 PACS number(s): 42.65.Es, 42.50.Hz

I. INTRODUCTION

Stimulated scattering of intense light is one of the major subjects in nonlinear optics. Although several types (Raman, Brillouin, Rayleigh wing, and thermal Rayleigh) of stimulated scattering were discovered in the 1960s, stimulated-scattering-related studies have remained highly active over the past several decades because of both the fundamental research interest and the potential applications [1–4]. First, stimulated scattering is one of the most effective physical approaches to generate frequency-shifted coherent light emission. Second, stimulated scattering is one of the most effective technical approaches to generate optical phase-conjugate waves. In addition, the study of various stimulated scattering effects can provide knowledge and useful information about the interaction between nonlinear scattering media and intense coherent light radiation.

So far, for all known stimulated scattering effects, there is always a frequency shift between the stimulated scattering beam and the pump laser beam. For example, the frequency shift values are large (10^2–10^3 cm^{-1}) for most stimulated Raman scattering processes that generally involve molecular vibrational transitions [5]. For backward stimulated Brillouin scattering in liquid and solid media, these values are quite small (10^{-1}–1 cm^{-1}), corresponding to frequencies of optoelectrostriction-induced hypersonic waves [6]. In addition, the reported frequency-shift values for stimulated Rayleigh-wing scattering were around several cm^{-1} [7], whereas they are more than several hundreds of cm^{-1} for stimulated Kerr scattering [8]. These two types of stimulated emission have been observed only in Kerr liquids consisting of anisotropic molecules, and the frequency-shift range is determined by the optical-field-induced reorientation property of anisotropic liquid molecules.

There is another relatively unexplored effect named stimulated thermal Rayleigh scattering [9,10], which was observed by Rank *et al.* and Cho *et al.* in linear absorbing media, and was explained by Herman and Gray using a theory of one-photon-absorption-enhanced thermal density fluctuation [11–13]. This theory could give an expression for the gain factor and predict an anti-Stokes shift that was about one-half of the pump spectral linewidth, provided that the pump laser linewidth is much greater than the linewidth of spontaneous Rayleigh scattering for a given scattering medium. Although this precondition is satisfied under most experimental conditions, there was a lack of experimental results to support the prediction of the anti-Stokes shift. Some early reports partially supported this prediction [9,10,14], whereas some others did not [15,16]. According to the same theory [11], considerable linear (one-photon) absorption is needed to enhance the thermal fluctuation of a given scattering medium; however, on the other hand, a considerable linear attenuation would be highly harmful for the initial "seed" (spontaneous) scattering signal. One needs to remember that all other types of stimulated scattering always require that the chosen gain (scattering) medium should exhibit as small a linear absorption as possible to lower the pump threshold of stimulated scattering. For this reason the so-called stimulated thermal Rayleigh scattering (STRS) might be quite difficult to observe, and that may be the reason why only a very small number of reports on this specific subject have appeared.

The possible two-photon absorption (2PA) contribution to the stimulated thermal scattering in pure organic solvents (such as benzene) was first reported by Boissel *et al.* [17], although there was a lack of specific identification of the observed stimulated scattering. Later, the same possibility was also mentioned by Karpov *et al.* in another experimental

study using organic solvents (such as hexane) as the scattering media to generate backward STRS [18].

Since 1995 we have been involved in studies of multiphoton excitation processes and multiphoton absorbing materials [19–23]. While measuring the 2PA cross section (σ_2) values of some two-photon active chromophore-solution samples via the nonlinear transmission method, it has been found that the 2PA cross-section value measured with a focused laser beam at a given wavelength and with nanosecond pulse duration is not a constant. Specifically, when the input laser intensity is higher than a certain (threshold) value, the measured 2PA cross-section values increase with increasing input laser intensity. This unexpected increase of apparent cross-section values for a given sample can be explained if we assume there are some additional nonlinear processes which may take energy from the input laser beam and cause the additional decrease of the nonlinear transmission. One possible effect is excited-state absorption. The other might be a backward stimulated scattering process related to 2PA. Experimentally, after putting a beam splitter on the backward side of the cuvette containing the 2PA solution sample, we indeed could see a highly directional backward stimulated scattering beam, provided that the intensity of the input laser beam and the 2PA coefficient (β) of the sample medium were high enough. After pursuing thorough measurements and specially designed experiments, it is found that the wavelength of such observed backward stimulated scattering is exactly the same as that of the input pump laser, and the feedback mechanism of the stimulated scattering observed in our experiments is mainly provided by the reflection from a stationary Bragg grating formed by the forward pump beam and backward Rayleigh scattering beam. For this reason it seems appropriate to term this specific effect stimulated Rayleigh-Bragg scattering (SRBS) in two-photon absorbing media.

This paper is organized as follows. (i) In Sec. II we provide a brief description of the basic experimental results on this specific stimulated scattering effect. (ii) In Sec. III we present a brief theoretical analysis based on a modified Herman and Gray theory by considering 2PA-enhanced thermal density fluctuations, the results of which are compared with the experiments. (iii) In Sec. IV we describe a 2PA-enhanced Bragg grating feedback model in detail, and present the experimental results that quantitatively supported this theoretical model.

II. EXPERIMENTAL MANIFESTATION OF STIMULATED RAYLEIGH-BRAGG SCATTERING

Even though all experimental results presented in this paper are based on a particular two-photon absorbing chromophore solution, namely, a dye named PRL 802 in tetrahydrofuran (THF) at 0.01*M* concentration [24], we believe that the discussed effect is applicable to all two-photon absorbing media. In our specific experiment, a 1-cm path length solution sample was pumped by a focused 532-nm laser beam that was generated from a frequency-doubled and *Q*-switched neodymium doped yttrium aluminum garnet (Nd:YAG) laser working at a variable repetition rate from 1 to 10 Hz. The laser pulse duration was ~10 ns when utilizing either a Pockels' cell as the active *Q*-switching element or a BDN-doped polymer sheet as the passive *Q*-switching element. The spectral linewidth of the 532-nm laser output was either $\sim 0.8\ \mathrm{cm}^{-1}$ in the former case or $\sim 0.08\ \mathrm{cm}^{-1}$ in the latter case. The 2PA coefficient of the sample solution of 0.01*M* was measured to be $\beta \approx 9.46\ \mathrm{cm/GW}$ when the input laser pulse energy (or intensity) was kept lower than ~60 μJ (or $\sim 40\ \mathrm{MW/cm}^2$). The observed features of this stimulated scattering phenomenon can be summarized as follows.

(1) *Threshold property*: with a focusing lens of $f = 10$ cm, the threshold pump energy (or intensity) value was measured to be ~60 μJ (or $40\ \mathrm{MW/cm}^2$) for passively *Q*-switched laser pulses, which was much lower than the threshold value ($\geqslant 150\ \mu$J or $100\ \mathrm{MW/cm}^2$) of backward stimulated Brillouin scattering in a 1-cm-long pure THF sample under the same conditions.

(2) *High directionality*: the stimulated scattering can be observed only in the exact backward direction with nearly the same beam divergence as the input pump laser beam (~1 mrad).

(3) *Spectral identity*: the measured central peak wavelength of the backward stimulated scattering is exactly the same as the input pump laser within a spectral resolution better than half of the input laser linewidth.

(4) *Temporal behavior*: the measured pulse duration of backward stimulated scattering is always shorter or considerably shorter than that of the input pump laser pulses.

Among all of the above-mentioned properties, the most special feature is that under our experimental conditions, there is no frequency shift between the pump laser beam and the backward stimulated Rayleigh-Bragg scattering beam. This feature has been demonstrated by using 532-nm laser beams with narrow spectral linewidth of $\sim 0.08\ \mathrm{cm}^{-1}$ and broad spectral linewidth of $\sim 0.8\ \mathrm{cm}^{-1}$, respectively. For the case of a narrow ($\sim 0.08\ \mathrm{cm}^{-1}$) pump laser line, this measurement was performed by using a 10-mm-spacing Fabry-Pérot interferometer, which showed no wavelength shift for backward stimulated scattering within the spectral resolution of $\sim 0.025\ \mathrm{cm}^{-1}$ [24]. For the case of a broad ($\sim 0.8\ \mathrm{cm}^{-1}$) pump laser line, the spectral measurement was conducted by using a 1-m double monochromator (from Jobin-Yvon) in conjunction with a charge-coupled-device camera system. The spectral resolution of our system was determined to be $\sim 0.11\ \mathrm{cm}^{-1}$, which was calibrated by using an extremely narrow 532-nm laser line with a spectral width less than $0.005\ \mathrm{cm}^{-1}$, generated from a seeded single-longitudinal-mode Nd:YAG laser (PRO-230, from Spectra-Physics). The spectral photographs for the input pump line, the output backward SRBS line, and both lines together are shown in Fig. 1. Once again, there is no measured frequency shift within our spectral resolution which was much smaller than half of the pump laser linewidth.

Regarding this frequency-unshifted feature, two questions may arise. The first is whether or not we could explain the effect by using a previous theoretical model. If the answer is negative, then we have another question: can we explain our observation by using a different theoretical model? In the following two sections, we shall try to answer these two questions separately.

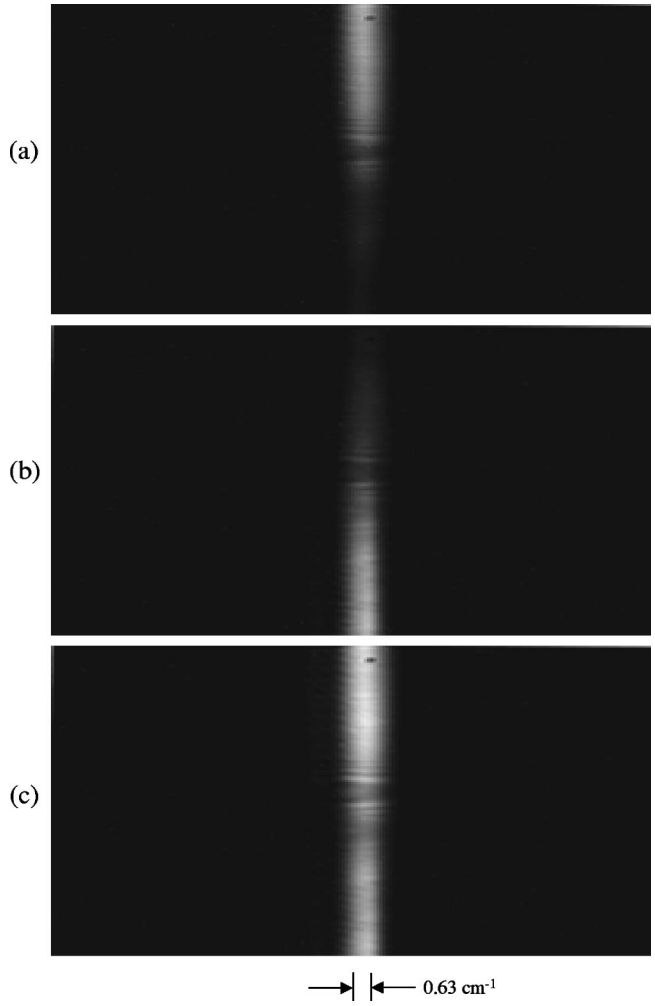

FIG. 1. Spectral photographs of (a) backward stimulated scattering, (b) input 532-nm pump laser, and (c) both stimulated scattering and pump laser. Spectral resolution: 0.11 cm^{-1}.

III. A MODIFIED PREVIOUS THERMAL DENSITY FLUCTUATION MODEL

In 1967, Herman and Gray reported a theoretical analysis based on a linear-absorption-enhanced thermal temperature and density fluctuation model [11], to explain the experimental observation of stimulated thermal Rayleigh scattering in a one-photon absorbing medium [9]. Now, one may wonder if the same theoretical frame is applicable to a two-photon absorbing scattering medium. For this reason, we try to modify their theory to consider thermal temperature and density fluctuations, which are enhanced by 2PA instead of linear absorption. To do so, we first give a set of equations [11,4]

$$\frac{\partial^2}{\partial t^2}\overline{\rho} - \frac{c_0^2}{\gamma}\nabla^2\overline{\rho} - \frac{\eta}{\rho_0}\frac{\partial}{\partial t}\nabla^2\overline{\rho} - \frac{c_0^2\beta_T\rho_0}{\gamma}\nabla^2\overline{T} = -\frac{\gamma^e}{8\pi}\nabla^2 E^2, \tag{1}$$

$$\rho_0 C_v\frac{\partial\overline{T}}{\partial t} - \lambda_T\nabla^2\overline{T} - \frac{C_v(\gamma-1)}{\beta_T}\frac{\partial\overline{\rho}}{\partial t} = \left(\frac{n_0 c}{4\pi}\right)^2\beta E^4, \tag{2}$$

where $\overline{\rho}$ and $\overline{T}$ are the density and temperature fluctuations of the scattering medium, ρ_0 is the average or unperturbed density, $\gamma^e=\rho_0(\partial\varepsilon/\partial\rho)_T$ is the electrostrictive coupling coefficient, $\gamma=C_p/C_v$ is the ratio of the specific heats at constant pressure and volume, λ_T and β_T are the coefficients of heat conduction and thermal expansion at constant pressure, η is the bulk viscosity coefficient, β is the two-photon absorption coefficient, n_0 is the refractive index, c_0 is the velocity of sound, c is the speed of light, and E is the optical electric field applied to the medium. Here, Eq. (1) describes the medium density fluctuation induced by the optoelectrostrictive effect, whereas Eq. (2) represents the temperature and density fluctuations enhanced by 2PA with the assumption that the linear (one-photon) absorption is negligible. The overall optical field may be regarded as a superposition of two waves, i.e., the input laser field E_L and the backward stimulated scattering field E_S:

$$E_L(z,t) = \frac{1}{2}\{E_L\exp[i(k_L z-\omega_L t)] + E_L^*\exp[-i(k_L z-\omega_L t)]\}, \tag{3}$$

$$E_S(z,t) = \frac{1}{2}\{E_S\exp[-i(k_S z+\omega_S t)] + E_S^*\exp[i(k_S z+\omega_S t)]\}; \tag{4}$$

meanwhile the fluctuating density and temperature can be written as

$$\overline{\rho} = \frac{1}{2}\{\rho\exp[i(kz-\omega t)] + \rho^*\exp[-i(kz-\omega t)]\}, \tag{5}$$

$$\overline{T} = \frac{1}{2}\{T\exp[i(kz-\omega t)] + T^*\exp[-i(kz-\omega t)]\}, \tag{6}$$

where $\omega=\omega_L-\omega_S$ is the frequency shift and $k=k_L+k_S$ is the sum of magnitudes of wave vectors for the two waves.

Substituting Eqs. (3)–(6) into Eqs. (1) and (2) leads to a steady-state solution for $\overline{\rho}$, and the presence of a gain for backward scattering field can be shown by solving the following steady-state nonlinear coupled wave equations through a procedure similar to that given by Herman and Gray:

$$\frac{dI_L}{dz} = -g_e I_L I_S - g_\beta I_L^2 I_S - \beta I_L^2, \tag{7}$$

$$\frac{dI_S}{dz} = -g_e I_L I_S - g_\beta I_L^2 I_S. \tag{8}$$

The above two equations describe the spatial attenuation for the forward pump laser intensity I_L, and the gain for the backward stimulated scattering intensity I_S, respectively. The gain factors for the latter can be expressed as

$$g_e = \frac{(\gamma-1)(\gamma^e)^2\omega_L\Gamma_R}{4c^2 n_0^2 c_0^2\rho_0}\frac{\omega}{\omega^2+(\Gamma_R/2)^2}, \tag{9}$$

$$g_\beta = -\frac{2\gamma^e \omega_L \beta_T \beta}{c n_0 \rho_0 C_p} \frac{\omega}{\omega^2 + (\Gamma_R/2)^2}, \tag{10}$$

where Γ_R is the spontaneous Rayleigh linewidth. Here, g_e is provided by the optoelectrostrictive mechanism, and g_β is provided by the 2PA mechanism. It can be seen that the signs of these two factors are opposite for a given frequency shift ω value. From Eq. (8) one can see that under the conditions of negligible linear absorption and pump intensity depletion, a small backward scattering signal will experience an exponential gain characterized by the following gain coefficient (in units of cm^{-1}):

$$G = g_e I_L^0 + g_\beta (I_L^0)^2, \tag{11}$$

where I_L^0 is the initial or undeleted pump intensity. If the input pump intensity is high enough the second gain term may become dominant and, therefore, we should only consider this term in detail.

According to Eq. (10), the spectral profile of the gain factor related to a 2PA contribution can be rewritten as

$$g_\beta = g_\beta^{\max} \frac{(\omega_S - \omega_L)\Gamma_R}{(\omega_S - \omega_L)^2 + (\Gamma_R/2)^2}, \tag{12}$$

where the maximum spectral gain factor is determined by

$$g_\beta^{\max} = -\frac{2\gamma^e \omega_L \beta_T}{c n_0 \rho_0 C_p} \frac{\beta}{\Gamma_R}, \tag{13}$$

which is proportional to the 2PA coefficient β and inversely proportional to the spontaneous Rayleigh linewidth Γ_R. A typical spectral gain profile determined by Eq. (12) is shown in Fig. 2(a) by the solid-line curve which indicates that the maximum gain will be reached at the position of $\Delta\omega = \omega_S - \omega_L = \Gamma_R/2$ on the anti-Stokes side of the pump wavelength.

Until now we have assumed that the input pump light is a monochromatic optical field. In reality, however, the input pump laser linewidth under most experimental conditions is orders of magnitude broader than the spontaneous Rayleigh linewidth, $\Gamma_R/2\pi$, which is around 20 MHz or 7×10^{-4} cm^{-1} for common optical media in the liquid phase. For instance, under our experimental conditions the pump laser linewidth was ~0.08 or ~0.8 cm^{-1}, depending on what type of *Q*-switching element was used. In both cases, we can treat the total input laser field as a superposition of a great number of different monochromatic spectral components. Each spectral component may produce its own gain curve and the summation of a greater number of them will lead to a severe cancellation of gain among them. For example, in Fig. 2(a) the dashed line shows the gain curve created by another input spectral component, the maximum gain position of which is just overlapping with the maximum attenuation position of the solid-line curve.

Mathematically, the overall gain profile for a given spectral distribution of pump field can be expressed as a convolution with the following form:

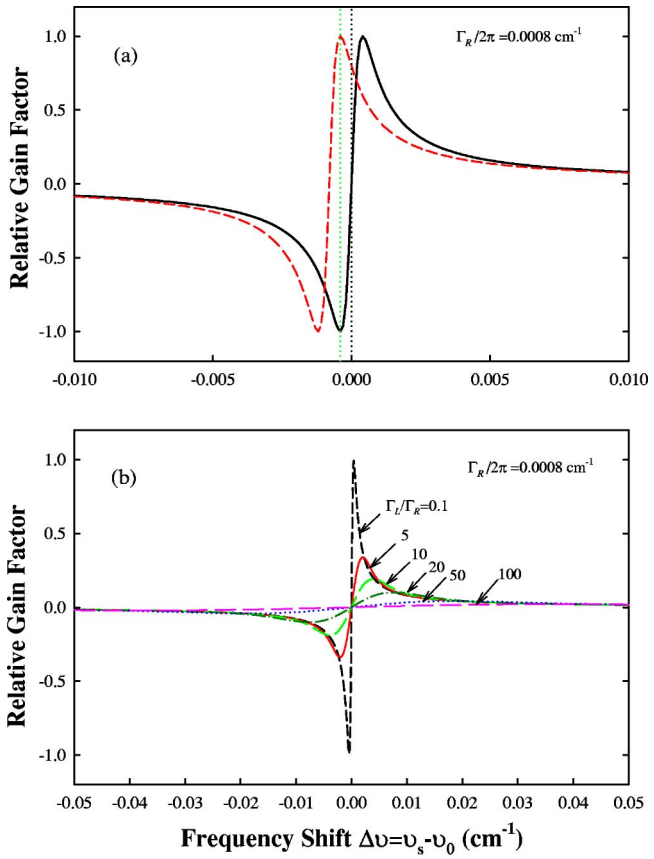

FIG. 2. (Color) (a) Relative gain factor as a function of frequency shift for two monochromatic pump components; (b) overall gain factor as a function of frequency shift at six different spectral linewidth ratios of Γ_L/Γ_R.

$$g_\beta^\Sigma(\omega_S - \omega_0) = \int_{-\infty}^{\infty} g_\beta^{\max} \frac{(\omega_S - \omega)\Gamma_R}{(\omega_S - \omega)^2 + (\Gamma_R/2)^2} F(\omega - \omega_0) d\omega, \tag{14}$$

where ω_0 is the central frequency of the pump laser spectrum with a given spectral profile function $F(\omega - \omega_0)$.

In general, Eq. (14) is not analytically solvable but can be solved numerically. To do so, we assume the pump laser exhibits a Gaussian spectral distribution with a given linewidth of Γ_L. The overall relative gain profiles given by numerical solutions of Eq. (14) are shown in Fig. 2(b) for six different values of (Γ_L/Γ_R), respectively. From Fig. 2(b) one can reach the following two conclusions: (i) the peak of the overall gain would be always located on the anti-Stokes side and near to the $(\Gamma_L/2)$ position, and (ii) when $\Gamma_L/\Gamma_R \gg 1$ the overall gain factor for a broader pump laser line is significantly smaller than that for a narrower pump line. The first conclusion is not supported by our experimental observation. On the other hand, the measured pump energy threshold values for observing backward SRBS were ~60 and ~58 μJ for pump linewidths of ~0.08 and ~0.8 cm^{-1}, respectively. This fact is obviously in contradiction with the second conclusion described above. Therefore we have to say that the modified Herman and Gray theory is not a suitable model to explain our experimental results.

IV. 2PA-ENHANCED BRAGG GRATING REFLECTION MODEL

In this section we suggest a two-photon-excitation-enhanced Bragg grating reflection model to explain the gain mechanism responsible for the backward frequency-unshifted Rayleigh scattering. It is well known that for any type of stimulated scattering the two basic requirements must be satisfied: (i) there is an original seed signal usually from the corresponding spontaneous scattering; (ii) there is a gain (or positive feedback) mechanism that ensures the further amplification of the original seed signals. In our case, the backward propagating spontaneous Rayleigh scattering can be thought of as an original seed signal that may interfere with the forward propagating pump wave to form a standing wave with a spatially modulated periodic intensity distribution. This intensity modulation may further induce an intensity-dependent refractive-index change and create a stationary Bragg grating [25]. A Bragg grating formed in such a way will offer a nonzero reflectivity for both the strong forward pump beam and the very weak backward scattering beam. However, the absolute value of the energy reflected from the pump beam to the scattering beam will be much greater than that from backward scattering beam to the pump beam. As a net result the backward scattering seed beam becomes stronger. Moreover, a slightly stronger backward scattering seed beam will enhance the modulation depth of the Bragg grating and consequently increase the reflectivity of this grating, which means more energy will transfer from the pump beam to the backward scattering beam. These processes may finally cause the backward scattering signals to be stimulated. One can see that there is a typical positive feedback provided by a stationary Bragg grating formed by two counterpropagating beams. With this assumption, 2PA may play a particularly important role in the following two senses. First, accompanying with 2PA there is a resonance-enhanced refractive-index change that is necessary for forming an effective Bragg grating [26–28]. Second, 2PA leads to a certain attenuation mainly on the strong pump beam, not on the much weaker seed scattering beam. In contrast, for a linear absorbing medium, the linear attenuation ratio is the same for both strong pump beam and weak scattering beam, which may prohibit the latter from being completely stimulated. That can explain why the effect of frequency-unshifted stimulated Rayleigh scattering is much easier to observe in a two-photon absorbing medium than in a linear absorbing medium.

To give a mathematical description for the suggested Bragg grating model, we can write the intensity of the overall optical field inside the scattering medium as

$$I(z) = (I_L + I_S) + 2\sqrt{I_L I_S}\cos(4\pi n_0 z/\lambda_0). \tag{15}$$

Here I_L is the intensity of the forward pump beam, I_S the intensity of backward Rayleigh scattering beam, and n_0 is the linear refractive index of the scattering medium at λ_0. This periodic intensity modification will produce a refractive-index change with the same spatial period $(n_0\lambda_0/2)$ due to the third-order nonlinear polarization effect. The spatial modulation of the intensity-dependent refractive-index change can be expressed as

$$\Delta n(z) = n_2 \Delta I(z) = 2n_2\sqrt{I_L I_S}\cos(4\pi n_0 z/\lambda_0) = \delta n \cos(4\pi n_0 z/\lambda_0). \tag{16}$$

Here n_2 is the nonlinear refractive-index coefficient, the value of which for a given medium is dependent on the specific mechanism of induced refractive-index change; δn is the amplitude of the spatial refractive-index modulation. Since the scattering medium is two-photon absorbing, the nonlinear refractive-index coefficient n_2 can be significantly enhanced due to resonant interaction between the laser field and the nonlinear medium, as described by [3]

$$n_2(\omega_0) \propto d_0\sigma_2 \frac{\omega_{2PA} - 2\omega_0}{(\omega_{2PA} - 2\omega_0)^2 + (\Gamma_{2PA}/2)^2}, \tag{17}$$

where d_0 is the molar concentration of two-photon absorbing dye molecules, σ_2 is the molecular 2PA cross section, and ω_{2PA} and Γ_{2PA} are the central frequency and bandwidth of the 2PA spectrum for a given medium, respectively. From Eq. (17) it can be seen that $|n_2(\omega_0)|$ reaches its maximum value when $|\omega_{2PA} - 2\omega_0| \Rightarrow \Gamma_{2PA}/2$.

Light-induced periodic refractive-index changes inside a nonlinear medium may create an induced Bragg phase grating [25–28], which in turn provides an effective reflection for both beams by the same reflectivity R. In our experimental case, the laser-induced Bragg grating is essentially a thick hologram grating with a cosinusoidal spatial modulation, and its reflectivity is simply given by the well-known Kogelnik coupled wave theory of thick hologram gratings [29]:

$$R = \tanh^2(\pi\delta n L/\lambda_0). \tag{18}$$

Here L is the thickness of the grating or the effective gain length inside the scattering medium. From Eq. (16) we have

$$\delta n = 2n_2\sqrt{I_L I_s}.$$

Then Eq. (18) becomes

$$R = \tanh^2(2\pi n_2\sqrt{I_L I_S}L/\lambda_0). \tag{18′}$$

The threshold condition for stimulating the backward Rayleigh can be expressed as

$$RI_L \gg I_S\{1 - \exp[-\alpha(\lambda_0)L]\}, \tag{19}$$

where $\alpha(\lambda_0)$ is the residual linear attenuation coefficient at λ_0. Under the threshold condition, we can assume $R \ll 1$ and $\alpha(\lambda_0)L \ll 1$, the hyperbolic tangent function in Eq. (18′) can be replaced by its arguments and Eq. (19) can be finally simplified as

$$(2\pi n_2/\lambda_0)^2 L I_L^2 \geqslant \alpha(\lambda_0). \tag{19′}$$

The physical meaning of the above condition is that for a given pump intensity level of I_L, the backward stimulated Rayleigh-Bragg scattering is easier to be observed in a two-photon absorbing medium possessing a larger n_2 value, a longer gain length L, and a smaller optical attenuation.

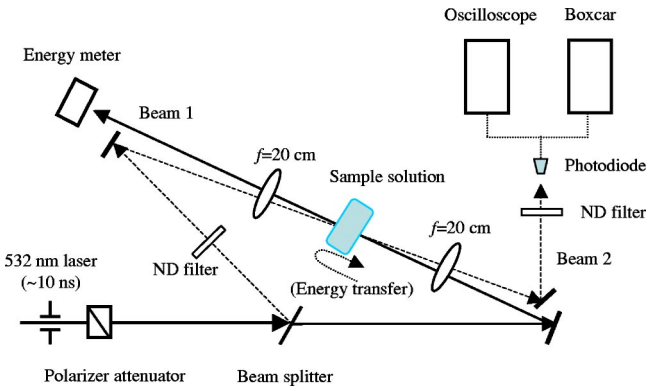

FIG. 3. (Color) Optical setup for two-counterpropagating-beam-induced Bragg grating experiment. ND indicates neutral density.

V. VERIFYING EXPERIMENT FOR THE BRAGG GRATING REFLECTION MODEL

To verify the validity of the above-described theoretical model of grating reflection, a specially designed two-counterpropagating-beam coupling experiment has been conducted. The experimental setup is shown in Fig. 3, where the 532-nm laser output of $\sim 0.8\text{-cm}^{-1}$ linewidth from the Pockels-cell-switched Nd:YAG laser was split into two counterpropagating beams: a strong pump beam 1 and a very weak probe beam 2 with a huge intensity difference (more than 600–6000 times). Both beams were focused through two lenses of $f=20$ cm onto the center of a 1-cm path-length cuvette filled with PRL 802 (0.01*M* in THF). The crossing angle of these two beams was 177.5°. The energy change of pump beam 1 was controlled by rotating a polarizer prism, and a change in intensity ratio between these two beams was achieved by using a variable neutral-density filter. The gain of beam 2 could be measured either by a boxcar averager (Model 4420 from Princeton Applied Research) or by a 500-MHz two-channel digital oscilloscope (Infinium from Hewlett Packard).

This experiment allows us to observe such a two-beam-induced Bragg grating and energy transfer from the strong beam 1 to the much weaker beam 2, owing to the reflection from the induced grating. As an illustration, Fig. 4 shows the measured gain behavior of beam 2 as a function of the energy of beam 1 under the condition of keeping the same intensity (energy) ratio of $\xi=I_2/I_1$. In Fig. 4, each data point represents an average over six pulses of the 532-nm laser with a repetition rate of 5 Hz. Based on the measured signal levels of beam 2 with and without interacting with beam 1, the relative gain of beam 2 as a function of energy of beam 1 can be easily determined. According to Eq. (18′) the energy transfer from beam 1 to 2 can be written as

$$\Delta I_1 = RI_1 \approx (2\pi n_2 L/\lambda_0)^2 I_1^2 I_2 \propto I_1^2 I_2. \tag{20}$$

If we assume the energy loss due to grating reflection for beam 2 is negligible because $R \ll 1$, the relative gain of beam 2 can be expressed as

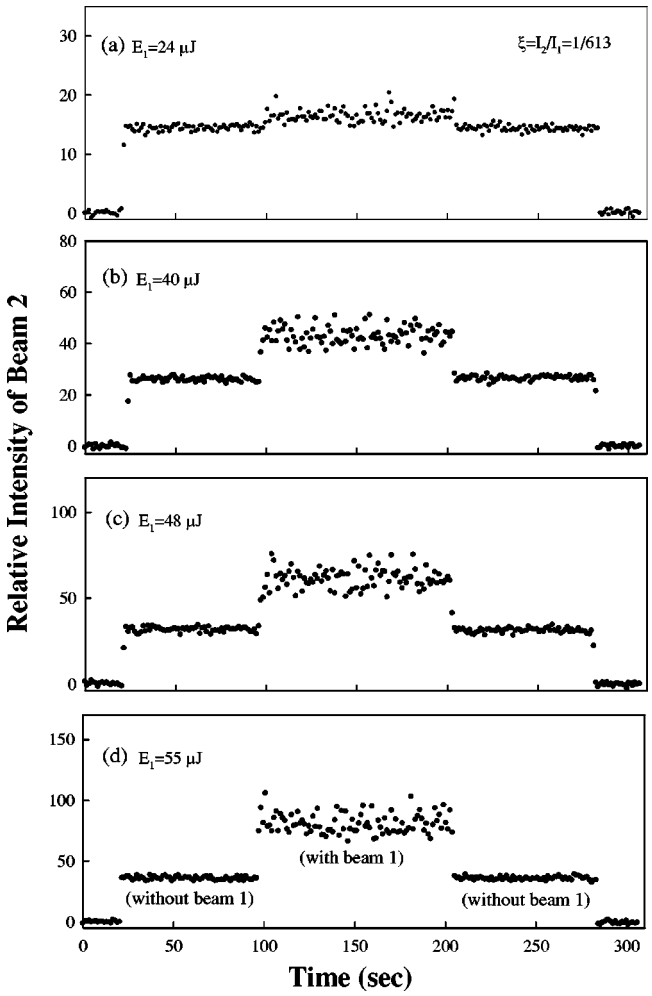

FIG. 4. Boxcar-averager-measured gain behaviors of a weak probe beam 2 at four different energy levels of a strong pump beam 1 under the condition of the same ratio of $I_2/I_1=1/613$.

$$G = \Delta I_1/I_2 \propto I_1^2. \tag{21}$$

This simple equation implies two important predictions: the gain G is (i) proportional to I_1^2 and (ii) independent of I_2, provided $I_1 \gg I_2$ and $R \ll 1$. The first prediction is proven by the results shown in Fig. 5, where the hollow circles represent the measured G values as a function of the energy values of beam 1, while the dashed line represents the fitting curve by using a square law, i.e., $y=ax^2$. To verify the second prediction, we have also measured the relative gain behavior of beam 2 at its different input energy values keeping the same energy (I_1) level for beam 1. The boxcar-measured gain behaviors are shown in Fig. 6, while the data finally obtained are shown in Fig. 7(a). From the latter figure we can see that the measured G values are basically independent of the I_2 values within the experimental uncertainty, which is an experimental proof of the second prediction mentioned above. Absolute values of the induced grating's reflectivity can also be determined through the measured gain values of beam 2. From Eqs. (20) and (21) we have

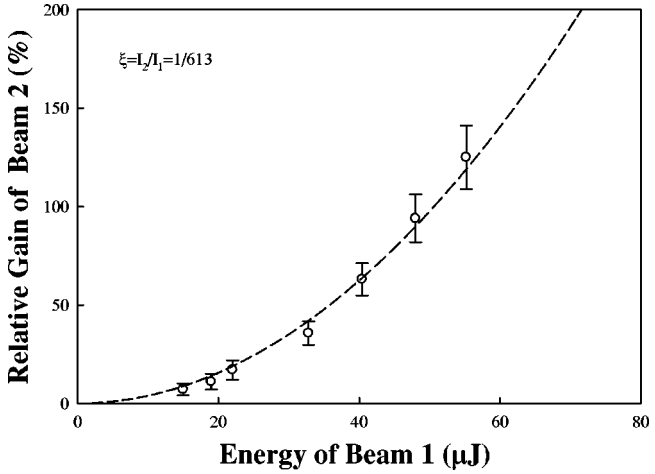

FIG. 5. Measured relative gain of beam 2 as a function of energy of beam 1 under the condition of the same ratio of $I_2/I_1 = 1/613$. The dashed line is a fitting curve using a square law.

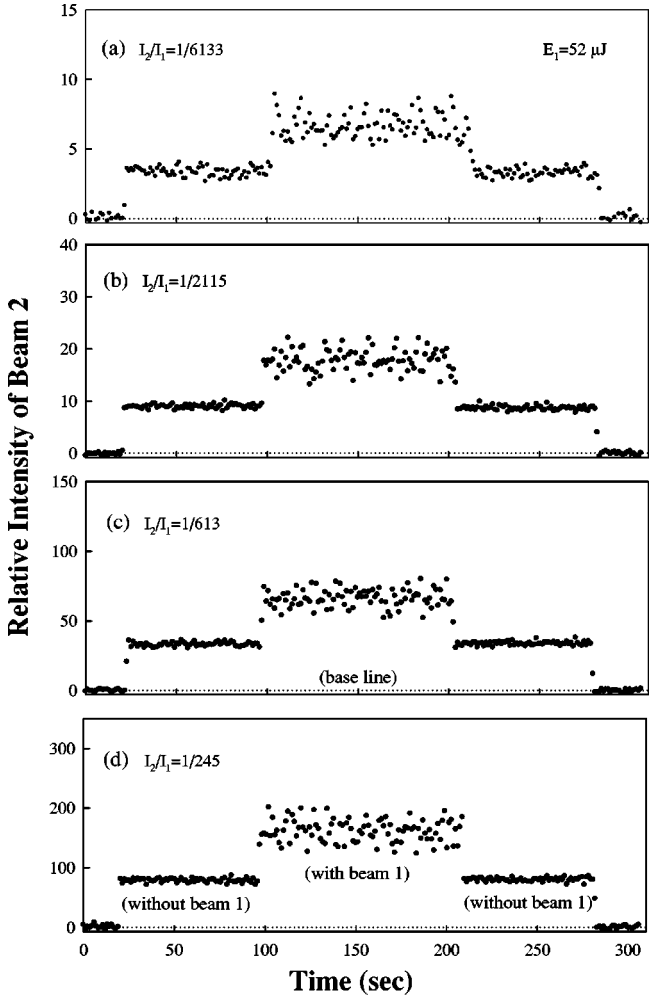

FIG. 6. Boxcar-averager-measured gain behaviors of beam 2 at four different ratios of I_2/I_1 under the condition of the same energy level of beam 1.

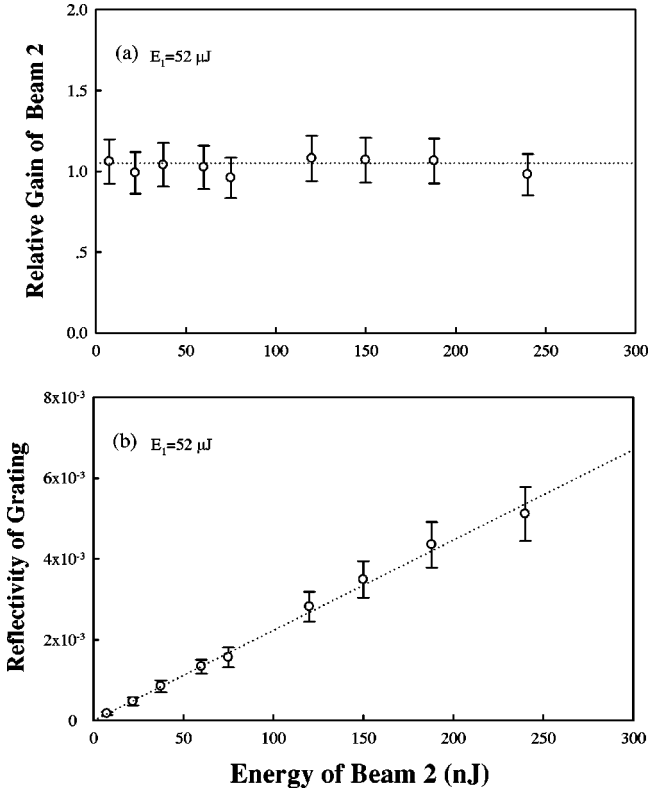

FIG. 7. Relative gain of beam 2 (a) and reflectivity of induced grating (b) as a function of the energy of beam 2 under the condition of the same energy level of beam 1.

$$R = \Delta I_1/I_1 = GI_2/I_1. \tag{22}$$

Based on the measured data shown in Fig. 7(a), we can finally display the values of reflectivity R in Fig. 7(b), as a function of I_2 under the condition of a fixed I_1. In this specific case, we see that the grating reflectivity R is proportional to the intensity (energy) of beam 2, as predicted by Eq. (22). As we mentioned before, an increase of the weak signal beam will further enhance the reflectivity and allow it to get still more energy from the strong pump beam. That is the positive feedback mechanism needed for generating stimulated scattering.

Alternatively, the gain behavior of weak beam 2 can also be measured by using a high-speed oscilloscope system shown in Fig. 3. In the case of utilizing a boxcar averager, the measured data were based on a double temporal average: first over a single laser pulse profile and then over six sequential laser pulses. In the case of utilizing an oscilloscope, we can record the dynamic gain behavior of even an individual laser pulse. In general, the 532-nm laser pulses from a Pockels-cell-switched Nd:YAG laser have a randomly fluctuating wave form and are poorly reproducible. This difficulty could be partially removed by utilizing a Pockels cell and a BDN dye-doped polymer sheet together to improve the regularity of the laser pulse shape. Figure 8 shows the simultaneously measured profiles of the input (dashed line) and output (solid line) pulses for beam 2 under this operation condition. To obtain the results shown in Fig. 8(a), the strong

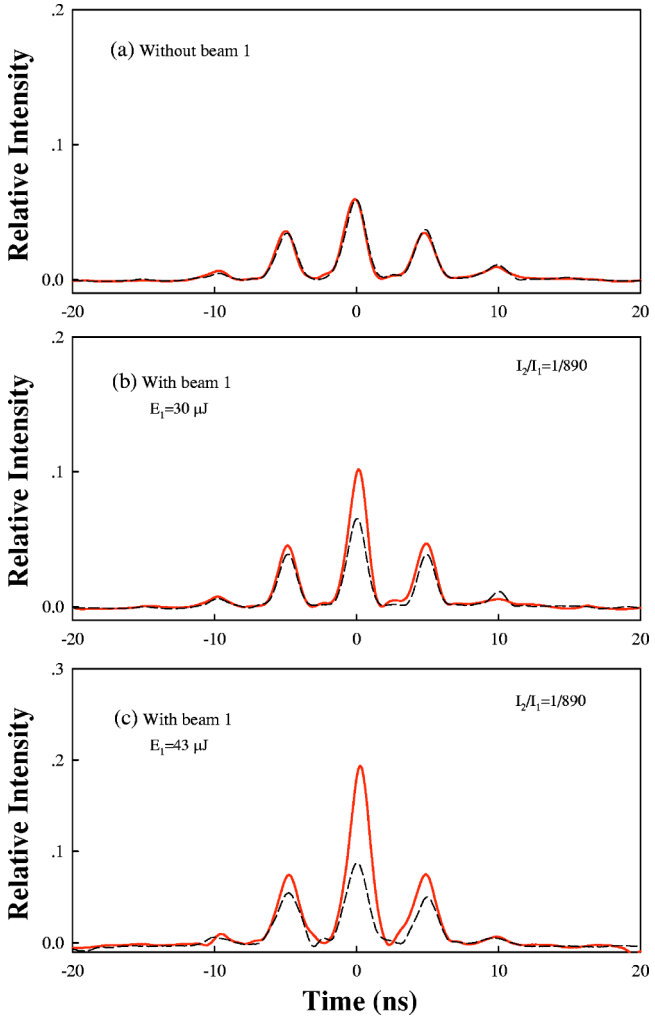

FIG. 8. (Color) Temporal profiles for the input (solid line) and output (dashed line) pulse of beam 2 at two different energy levels of beam 1: (a) beam 1 was blocked, (b) $E_1=30\ \mu$J, and (c) $E_1=43\ \mu$J under the condition of the same ratio of $I_2/I_1=1/890$.

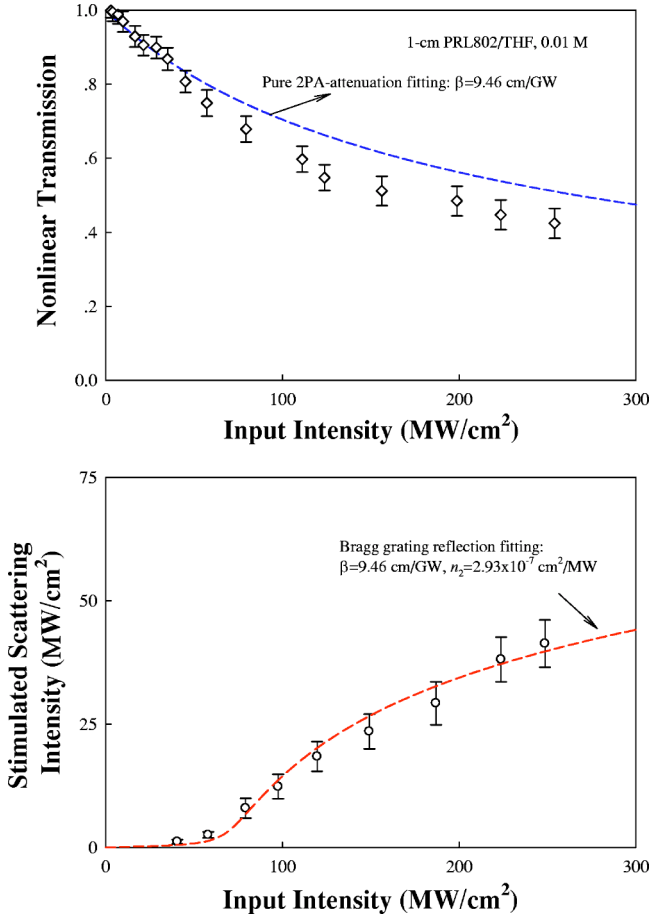

FIG. 9. (Color) (a) Measured nonlinear transmission of the pump beam vs input pump intensity; the dashed line is the best-fitting curve based on a pure 2PA process; (b) measured output backward stimulated scattering intensity vs input pump intensity; the dashed line is the best-fitting curve based on the grating reflection model.

beam 1 was blocked and there was no grating inside the nonlinear medium. Figures 8(b) and 8(c) clearly show the enhancement effect of beam 2 due to grating reflection at two different energy levels of beam 1. After subtracting the dashed-line curve from the solid-line curve we can finally obtain the dynamic information of the gain for beam 2 as a function of time. The remarkable features of the measured results shown in Figs. 8(b) and 8(c) are (i) the peak positions on the wave form for the amplified beam 2 are basically the same as that for the input pulse within our temporal resolution of ±0.5 ns; (ii) the amplified pulse shape of beam 2 remains symmetric like the input pulse. These two facts may imply a simplest case, i.e., a nearly instantaneous induced refractive-index change within the range of experimental uncertainty. Based on this assumption, the measured pulse shape of the amplified beam 2 can be well fitted by using a modified Eq. (21):

$$G(t) = \Delta I_1(t)/I_2(t) \propto I_1^2(t). \tag{23}$$

Here it should be noted that the relative pulse shapes for beams 1 and 2 are identical as they are from the same source.

To further verify the validity of the proposed physical model of grating reflection, we try to employ this model to fit the measured output-input relationship between the pump field and the stimulated scattering field. In Fig. 9(a) the diamond points represent the measured nonlinear transmission values as a function of the pump intensity. Here, the attenuation of the pump beam is due to a pure 2PA process when the pump level is lower than the threshold of stimulated scattering, then is due to both 2PA and backward stimulated scattering when the pump level is higher than the threshold. The best-fitting curve for the pure 2PA process is obtained by assuming 2PA coefficient $\beta=9.46$ cm/GW. In Fig. 9(b) the circle points represent the measured output intensity values of the backward stimulated scattering as a function of the input pump intensity. To fit the output-input relationship shown in Fig. 9(b), we can use an average approximation, i.e., to determine the grating reflectivity by estimating the average local intensity for the two beams at the central position of the gain medium. To do so, we first give the following expression for the average pump intensity inside the medium after considering 2PA-induced attenuation and the additional loss due to the grating reflection,

$$I_1' = I_1^0 \frac{\ln(1+\beta I_1^0 L/2)}{\beta I_1^0 L/2} T_0(1-R/2). \quad (24)$$

Here I_1^0 is the input pump intensity, β is the 2PA coefficient of the scattering medium, L is the path length of the sample solution, T_0 is the linear transmission passing through $L/2$ of the medium, and R is the average reflectivity of the induced Bragg grating. The average intensity of the backward stimulated scattering inside the medium can be written as

$$I_2' = I_1' R(1-R/2). \quad (25)$$

According to Eq. (18′), we have

$$R = \tanh^2[(\pi n_2 L/\lambda_0)\sqrt{I_1' I_2'}]. \quad (26)$$

Substituting Eq. (26) into Eqs. (24) and (25) provides a numerical solution for I_2', and the final output intensity of the backward stimulated scattering can be modified as

$$I_2 = I_2' \frac{\ln(1+\beta I_2' L/2)}{\beta I_2' L/2} T_0. \quad (27)$$

In our experimental condition, $L=1$ cm, $T_0 \approx 0.95$ (due to one window's reflection and residual linear attenuation), and $\beta = 9.46$ cm/GW. Then we can use these values and the above expression to fit the experimental data. The fitting curve is shown in Fig. 9(b) by a dashed line with a best-fitting parameter of $n_2 = 2.93 \times 10^{-7}$ cm^2/MW. From Fig. 9(b) one can see that the theoretical output-input relationship predicted by the grating reflection model is in fairly good agreement with the measured data within our experimental uncertainty.

VI. CONCLUSIONS

We have experimentally and theoretically studied backward stimulated Rayleigh-Bragg scattering in a two-photon absorbing dye solution. There are two salient experimental features that are different from other known stimulated scattering effects: (i) there is no measured frequency shift within a spectral resolution better than one-half of the pump laser linewidth; (ii) the measured pump threshold values are not dependent on the spectral linewidth (from 0.08 to 0.8 cm^{-1}) of the pump laser. These two features are not consistent with the predictions from a modified Herman and Gray theory considering the gain arising from two-photon-absorption-enhanced thermal density fluctuation. However, these two features can be well interpreted by a physical model of 2PA-enhanced Bragg grating reflection. This stationary Bragg grating is formed by a strong forward pump laser field and a much weaker backward Rayleigh scattering field of the same wavelength. The reflection from this stationary grating may substantially enhance the backward Rayleigh scattering and provides a positive feedback mechanism without causing any frequency shift. The two-photon absorbing medium may provide a resonance-enhanced refractive-index change to enhance the efficiency of the induced Bragg grating, while avoiding the harmful influence from linear absorption.

A specially designed two-counterpropagating-beam coupling grating experiment in a two-photon absorbing dye solution is conducted. The measured dynamic behavior of Bragg grating and its reflection property are quantitatively consistent with predictions from the suggested grating reflection model. The major contribution to the Bragg grating is attributed to a nearly instantaneous refractive-index change in the nanosecond regime, whereas the thermal refractive-index change is not likely contributing to the stimulated scattering because of its slower time response [30,31].

ACKNOWLEDGMENTS

This work was supported by the Air Force Office of Scientific Research and the Air Force Research Laboratory, Materials and Manufacturing Directorate.

[1] Y. R. Shen, *The Principles of Nonlinear Optics* (Wiley, New York, 1984).
[2] R. W. Boyd, *Nonlinear Optics*, 2nd ed. (Academic, San Diego, 2002).
[3] G. S. He and S. H. Liu, *Physics of Nonlinear Optics* (World Scientific, Singapore, 2000).
[4] W. Kaiser and M. Maier, in *Laser Handbook*, edited by F. T. Arecchi and E. O. Schulz-DuBois (North-Holland, Amsterdam, 1972).
[5] G. Eckhardt, R. W. Hellwarth, F. J. McClung, S. E. Schwarz, D. Weiner, and E. J. Woodbury, Phys. Rev. Lett. **9**, 455 (1962).
[6] R. Y. Chiao, C. H. Townes, and B. P. Stoicheff, Phys. Rev. Lett. **12**, 592 (1964).
[7] D. I. Mash, V. V. Morozov, V. S. Starunov, and I. L. Fabelinskii, JETP Lett. **2**, 25 (1965).
[8] G. S. He and P. N. Prasad, Phys. Rev. A **41**, 2687 (1990).
[9] D. H. Rank, C. W. Cho, N. D. Foltz, and T. A. Wiggings, Phys. Rev. Lett. **19**, 828 (1967).
[10] C. W. Cho, N. D. Foltz, D. H. Rank, and T. A. Wiggins, Phys. Rev. **175**, 271 (1968).
[11] R. M. Herman and M. A. Gray, Phys. Rev. Lett. **19**, 824 (1967).
[12] M. A. Gray and R. M. Herman, Phys. Rev. **181**, 374 (1969).
[13] I. P. Batra and R. H. Enns, Phys. Rev. **185**, 396 (1969).
[14] D. Pohl, I. Reinhold, and W. Kaiser, Phys. Rev. Lett. **20**, 1141 (1968).
[15] V. I. Bespalov, A. M. Kubarev, and G. A. Pasmanik, Phys. Rev. Lett. **24**, 1274 (1970).
[16] K. Darée and W. Kaiser, Phys. Rev. Lett. **26**, 816 (1971).
[17] P. Boissel, G. Hauchecorne, F. Kerherve, and G. Mayer, J. Phys. (France) Lett. **39**, 319 (1978).
[18] V. B. Karpov, V. V. Korobkin, and D. A. Dolgolenko, Sov. J. Quantum Electron. **21**, 1235 (1991).
[19] G. S. He, G. C. Xu, P. N. Prasad, B. A. Reinhardt, J. C. Bhatt, R. McKellar, and A. G. Dillard, Opt. Lett. **20**, 435 (1995).

[20] G. S. He, L. Yuan, N. Cheng, J. D. Bhawalkar, P. N. Prasad, L. L. Brott, S. J. Clarson, and B. A. Reinhardt, J. Opt. Soc. Am. B **14**, 1079 (1997).
[21] G. S. He, J. Swiatkiewicz, Y. Jiang, P. N. Prasad, B. A. Reinhardt, L.-S. Tan, and R. Kannan, J. Phys. Chem. A **104**, 4805 (2000).
[22] G. S. He, P. P. Markowicz, T.-C. Lin, and P. N. Prasad, Nature (London) **415**, 767 (2002).
[23] G. S. He, T.-C. Lin, J. Dai, P. N. Prasad, R. Kannan, A. G. Dombroskie, R. Vaia, and L.-S. Tan, J. Chem. Phys. **120**, 5275 (2004).
[24] G. S. He, T.-C. Lin, and P. N. Prasad, Opt. Express **12**, 5952 (2004).
[25] R. G. Brewer and C. H. Townes, Phys. Rev. Lett. **18**, 196 (1967).
[26] K. O. Hill, Y. Fujii, D. C. Johnson, and B. S. Kawasaki, Appl. Phys. Lett. **32**, 647 (1978).
[27] V. Mizrahi, S. LaRochelle, G. I. Stegeman, and J. E. Sipe, Phys. Rev. A **43**, 433 (1991).
[28] B. Guo and D. Z. Anderson, Appl. Phys. Lett. **60**, 67 (1992).
[29] H. Kogelnik, Bell Syst. Tech. J. **48**, 2909 (1969).
[30] H. J. Hoffman, J. Opt. Soc. Am. B **3**, 253 (1986).
[31] I. C. Khoo and Y. Liang, Phys. Rev. E **62**, 6722 (2000).